Supporting Information

Ren et al. 10.1073/pnas.0911396107

SI Materials and Methods

Inverse Dynamics Analysis. The 3D marker coordinate data obtained from the motion analysis system were filtered using a fourth-order low-pass, zero-lag Butterworth digital filter with a cutoff frequency of 10 Hz (1). These data were used to define the parasagittal plane motions of the upper arm, forearm, forefoot, thigh, shank, and hindfoot segments, as well as the shoulder, elbow, wrist, hip, knee and ankle joints. The CoM motions of each segment were derived based on the distal and proximal joint position data and body segment property (BSP) data from cadaveric dissections. The CoM acceleration $\vec{a}_{segment}$ and the angular acceleration $\alpha_{segment}$ of each limb segment were calculated by a first-order finite differentiation method (1).

The BSP data for each body segment, including mass ($m_{segment}$), CoM position, and moment of inertia ($I_{segment}$), were estimated based on the 3D reconstruction of CT image data of five whole Asian elephant cadavers (and additional assorted segments of other individuals) using interactive 3D geometrical modeling software (2, 3). Additional material from individual limb segments of other cadaveric individuals was used, including five manus specimens, two shank specimens, two thigh specimens, and six pes specimens, to estimate the in vivo subjects' BSPs (Table S2).

For each segment, for all available data, we calculated the average of the segment mass (as % body mass), CoM (as % segment length from the proximal end), and moment of inertia (normalized by body mass), and multiplied these by known masses or segment lengths for the study subjects. Error in these BSP estimates will have only miniscule effects on our main calculations (2, 4).

We used a standard inverse dynamics method to calculate the resultant forces and moments at each limb joint in the parasagittal plane for each sample frame by taking into account of all of the gravitational and inertial effects (1, 5, 6). The joint forces were calculated as follows:

For the forelimb:

$$\begin{cases} \vec{F}_{wrist} = m_{manus}\cdot\left(\vec{a}_{manus} - \vec{g}\right) - \vec{F}_{forelimb} \\ \vec{F}_{elbow} = m_{forearm}\cdot\left(\vec{a}_{forearm} - \vec{g}\right) + \vec{F}_{wrist} \\ \vec{F}_{shoulder} = m_{upperarm}\cdot\left(\vec{a}_{upperarm} - \vec{g}\right) + \vec{F}_{elbow} \end{cases}.$$

For the hindlimb:

$$\begin{cases} \vec{F}_{ankle} = m_{pes}\cdot\left(\vec{a}_{pes} - \vec{g}\right) - \vec{F}_{hindlimb} \\ \vec{F}_{knee} = m_{shank}\cdot\left(\vec{a}_{shank} - \vec{g}\right) + \vec{F}_{ankle} \\ \vec{F}_{hip} = m_{thigh}\cdot\left(\vec{a}_{thigh} - \vec{g}\right) + \vec{F}_{knee} \end{cases}.$$

Here $\vec{g}$ is the gravitational acceleration vector in the parasagittal plane. The net muscle moments at each limb joints were derived as follows:

For the forelimb:

$$\begin{cases} M_{wrist} = I_{manus}\cdot\alpha_{manus} - F_{wrist}\cdot r_{wrist,manus} - F_{forelimb}\cdot r_{ground,manus} \\ \qquad - M_{forelimb} \\ M_{elbow} = I_{forearm}\cdot\alpha_{forearm} + M_{wrist} - F_{elbow}\cdot r_{elbow,forearm} \\ \qquad + F_{wrist}\cdot r_{wrist,forearm} \\ M_{shoulder} = I_{upperarm}\cdot\alpha_{upperarm} + M_{elbow} - F_{shoulder}\cdot r_{shoulder,upperarm} \\ \qquad + F_{elbow}\cdot r_{elbow,upperarm} \end{cases}.$$

For the hindlimb:

$$\begin{cases} M_{ankle} = I_{pes}\cdot\alpha_{pes} - F_{ankle}\cdot r_{ankle,pes} - F_{hindlimb}\cdot r_{ground,pes} \\ \qquad - M_{hindlimb} \\ M_{knee} = I_{shank}\cdot\alpha_{shank} + M_{ankle} - F_{knee}\cdot r_{knee,shank} \\ \qquad + F_{ankle}\cdot r_{ankle,shank} \\ M_{hip} = I_{thigh}\cdot\alpha_{thigh} + M_{knee} - F_{hip}\cdot r_{hip,thigh} + F_{knee}\cdot r_{knee,thigh} \end{cases}.$$

Here $r_{i,j}$ is the moment arm of the joint force at joint i with respect to the CoM of body segment j and M_{limb} is the ground reaction moment exerted on the animal's limb in the parasagittal plane (Fig. 2*A*).

Effective Muscle Advantage. Assuming that all limb muscles are uniarticular and that no cocontractions occur at any joint (thus underestimating EMA for proximal joints, as in other studies), the antigravity muscle force, F_{muscle}, at each joint was calculated as M_{joint}/r_{muscle} (Fig. 2*A*). The muscle moment arm, r_{muscle}, was calculated as the mean anatomic moment arm for all agonist muscles weighted by each muscle's physiological cross-sectional area (PCSA) (5), as follows. Five cadaveric specimens (Table S2) were dissected to measure the architecture (7, 8) of all major muscle groups, including muscle masses, fascicle lengths, and pennation angles (and thereby PCSAs), as well as muscle moment arms using the tendon travel method (9). For all six major limb joints (shoulder, elbow, wrist, hip, knee, and ankle), we then calculated mean fascicle lengths (weighted by PCSA) for the muscles with appropriate antigravity (e.g., extensor, plantarflexor) moment arms for each specimen. We also then calculated mean moment arms for the antigravity muscles using the best data from three specimens (identified as A, B, and D in Table S2) in representative limb joint angles (running with dimensionless speeds >1; ref. 10). This assumes constant muscle moment arms regardless of speed or posture, as in previous studies of EMA (6, 11–13), an assumption worth testing in future studies.

Because variation in fascicle lengths and moment arms among individuals was relatively small, we took the mean for all individuals and normalized it by body mass$^{0.33}$ (as in ref. 8). This normalization reduces linear dimensions to a dimensionless number and avoids errors introduced by using body dimensions with their own inherent allometry, such as limb or segment lengths. We then multiplied these mean normalized fascicle lengths and moment arms by our study subjects' actual body mass$^{0.33}$ to obtain subject-specific estimates for our calculations of EMA and V_{musc}.

We then calculated the EMA at each joint as the ratio of the limb's GRF impulse to the antigravity muscle force impulse over the duration of limb support (5). This normalized impulse provided a measure of the average muscle force required to exert 1 BW of force on the ground, which corresponds to the r_{muscle}/R_{GRF} relationship commonly described by the muscle EMA. Thus has the advantage of allowing a comparison of muscle force generation requirements with respect to the GRF over the entire period of limb support, including those instants when the GRF passes through the joint's center of rotation (5).

Active Muscle Volume and Locomotor Costs. To estimate elephant locomotor costs at different speeds, we calculated the mass-specific volume of muscle activated per distance traveled (5, 6, 13) for all elephants as

$$\frac{V_{musc}}{m_{body}} = \frac{1}{\sigma}\cdot\left(\frac{l_{fasc,ankle}}{EMA_{ankle}} + \frac{l_{fasc,knee}}{EMA_{knee}} + \frac{l_{fasc,hip}}{EMA_{hip}} + \frac{l_{fasc,wrist}}{EMA_{wrist}} + \frac{l_{fasc,elbow}}{EMA_{elbow}} + \frac{l_{fasc,shoulder}}{EMA_{shoulder}}\right)\cdot\frac{g}{L_{step}},$$

where σ is an assumed constant muscle stress, 20 N cm^{-2} (6, 14), and l_{fasc} is the length of the muscle fascicles. For each joint, l_{fasc} is calculated as the mean fascicle length for all agonist muscle groups weighted by each muscle's PCSA, and L_{step} is step length, the horizontal distance covered by the whole-body CoM during the stance phase.

To check the correlation of published metabolic costs for elephants (15) with our muscle recruitment–based cost estimates, we digitized the published data for net cost of transport, adjusted speeds to our dimensionless speeds (assuming hip heights of 1.5 m), and placed the data into the same speed categories as shown in Fig. 3. We then assumed the conventional 20.1 J = 1 mL O_2 conversion into oxygen consumption (6, 13, 16), and plotted the ordinary least squares regression of both data sets to obtain a linear relationship between them.

Locomotor costs are not determined simply by muscle recruitment, however; mechanical work is an important cost as well (2, 6, 13, 15-19). To compare these two kinds of costs and determine which have the best fit to metabolic data, we calculated total mechanical work for the same speed categories using our data (Fig. S4) for individual limb work, and also calculated work based solely on CoM motions (i.e., "external work," identical to the "combined limb method" (16, 17, 19). As expected, the former approach gave much higher (almost doubled) estimates of work (Table S4); however, both approaches fit the metabolic costs much worse than our muscle recruitment–based estimates (compare R^2 values in Table S4). Other likely costs, such as limb swinging, are not considered by any of these methods and merit investigation.

1. Winter DA (2005) *Biomechanics and Motor Control of Human Movement* (Wiley, New York), 3rd Ed.
2. Ren L, Hutchinson JR (2008) The three-dimensional locomotor dynamics of African (*Loxodonta Africana*) and Asian (*Elephas maximus*) elephants reveal a smooth gait transition at moderate speed. *J R Soc Interface* 5:195–211.
3. Allen V, Paxton H, Hutchinson JR (2009) Variation in center of mass estimates for extant sauropsids and its importance for reconstructing inertial properties of extinct archosaurs. *Anat Rec* 292:1442–1461.
4. Reinbolt JA, Haftka RT, Chmielewski TL, Fregley BJ (2007) Are patient-specific joint and inertial parameters necessary for accurate inverse dynamics analyses of gait? *IEEE Trans Biomed Eng* 54:782–793.
5. Biewener AA, Farley CT, Roberts TJ, Temaner M (2004) Muscle mechanical advantage of human walking and running: implications for energy cost. *J Appl Physiol* 97: 22662274.
6. Pontzer H, Raichlen DA, Sockol MD (2009) The metabolic cost of walking in humans, chimpanzees, and early hominins. *J Hum Evol* 56:43–54.
7. Calow LJ, Alexander RMcN (1973) A mechanical analysis of the hind leg of a frog (*Rana temporaria*). *J Zool* 171:293–321.
8. Payne RC, Hutchinson JR, Robilliard JJ, Wilson AM (2005) Functional specialisation of the equine pelvic limb. *J Anat* 206:557–574.
9. An KN, Takahasi K, Harrigan TP, Chao EY (1984) Determination of muscle orientations and moment arms. *J Biomech Eng* 106:280–282.
10. Ren L, et al. (2008) The movements of limb segments and joints during locomotion in African and Asian elephants. *J Exp Biol* 211:2735–2751.
11. Biewener AA (1990) Biomechanics of mammalian terrestrial locomotion. *Science* 250: 1097–1103.
12. Biewener AA (2005) Biomechanical consequences of scaling. *J Exp Biol* 208: 1665–1676.
13. Roberts TJ, Chen MS, Taylor CR (1998) Energetics of bipedal running, II: Limb design and running mechanics. *J Exp Biol* 201:2753–2762.
14. Hutchinson JR, Famini D, Lair R, Kram R (2003) Are fast-moving elephants really running? *Nature* 422:493–494.
15. Langman VA, et al. (1995) Moving cheaply: Energetics of walking in the African elephant. *J Exp Biol* 198:629–632.
16. Cavagna GA, Heglund NC, Taylor CR (1977) Mechanical work in terrestrial locomotion: Two basic mechanisms for minimizing energy expenditure. *Am J Physiol Regul Integr Comp Physiol* 233:R243–R261.
17. Genin JJ, Willems PA, Cavagna GA, Lair R, Heglund NC (2010) Biomechanics of locomotion in Asian elephants. *J Exp Biol* 213:694–706.
18. Rubenson J, Heliams DB, Lloyd DG, Fournier PA (2004) Gait selection in the ostrich: Mechanical and metabolic characteristics of walking and running with and without an aerial phase. *Proc R Soc Lond B Biol Sci* 271:1091–1099.
19. Donelan JM, Kram R, Kuo AD (2002) Simultaneous positive and negative external mechanical work in human walking. *J Biomech* 35:117–124.
20. Miller CE, Basu C, Fritsch G, Hildebrandt T, Hutchinson JR (2008) Ontogenetic scaling of foot musculoskeletal anatomy in elephants. *J R Soc Interface* 5:465–476.
21. Alexander RMcN, Jayes AS, Maloiy GMO, Wathuta EM (1981) Allometry of the leg muscles of mammals. *J Zool* 194:539–552.
22. Muybridge E (1899) *Animals in Motion* (Chapman & Hall, London).
23. Gambaryan PP (1974) *How Mammals Run* (Wiley, New York).
24. Hutchinson JR, et al. (2006) The locomotor kinematics of African and Asian elephants: Changes with speed and size. *J Exp Biol* 209:3812–3827.

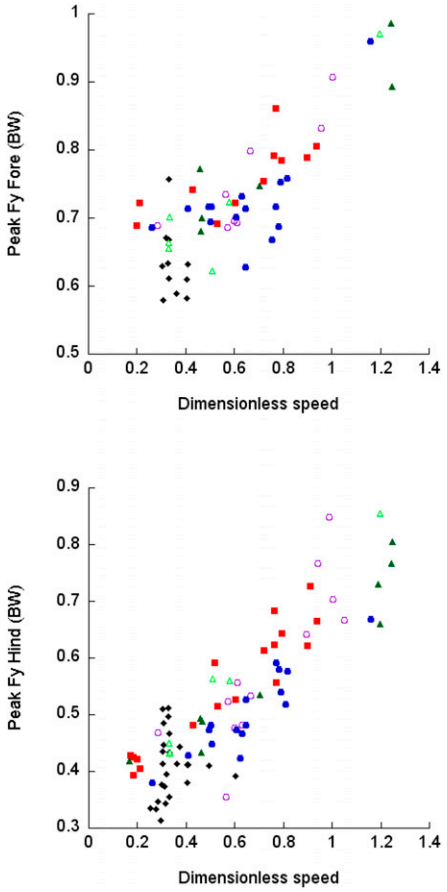

Fig. S1. Peak limb vertical forces (F_y; in multiples of body weight) versus dimensionless speed. Least squares linear regression data ($y = b + mx$, where b is the intercept and m is the slope) are as follows: forelimb, $n = 58$, $y = 0.558 + 0.283x$; $R^2 = 0.668$; $P < 0.01$; hindlimb, $n = 85$, $y = 0.295 + 0.380x$; $R^2 = 0.767$, $P < 0.01$. Symbols indicate data from different subjects.

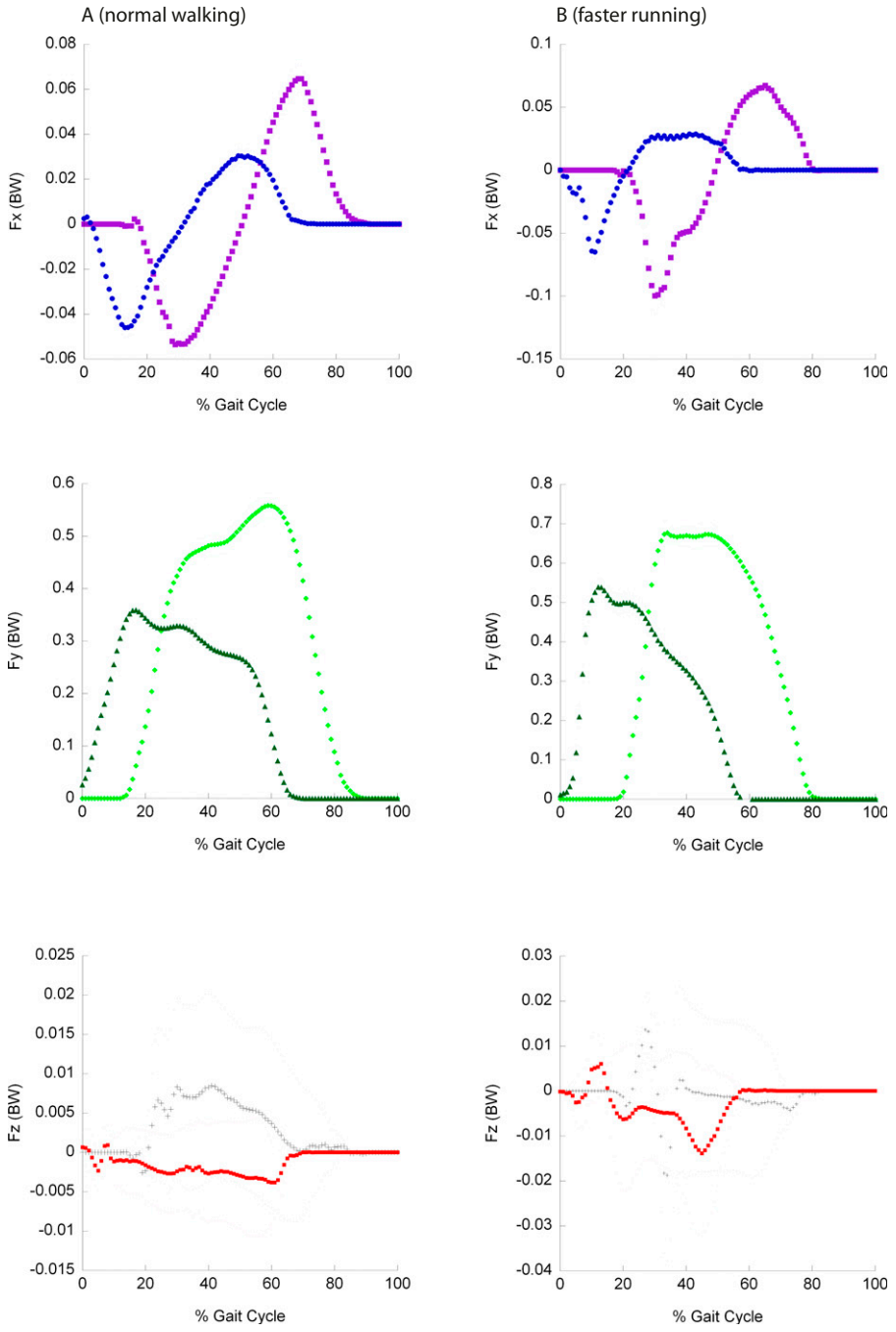

Fig. S2. Individual limb GRFs (in multiples of body weight) versus % gait cycle for (*A*) normal walking (dimensionless speed 0.30–0.35) and (*B*) faster running (dimensionless speed 0.75–1.3). These are expanded views of data in Fig. 1. F_x is the horizontal component (craniocaudal; purple squares, forelimb; blue circles, hindlimb), and F_y is the vertical component (light-green diamonds, forelimb; dark-green triangles, hindlimb). Also included are data for the mediolateral component (F_z) (black crosses, forelimb; red squares, hindlimb) and ± SEM values (small points, sometimes obscured by larger mean data points; zoom into image for clearest view).

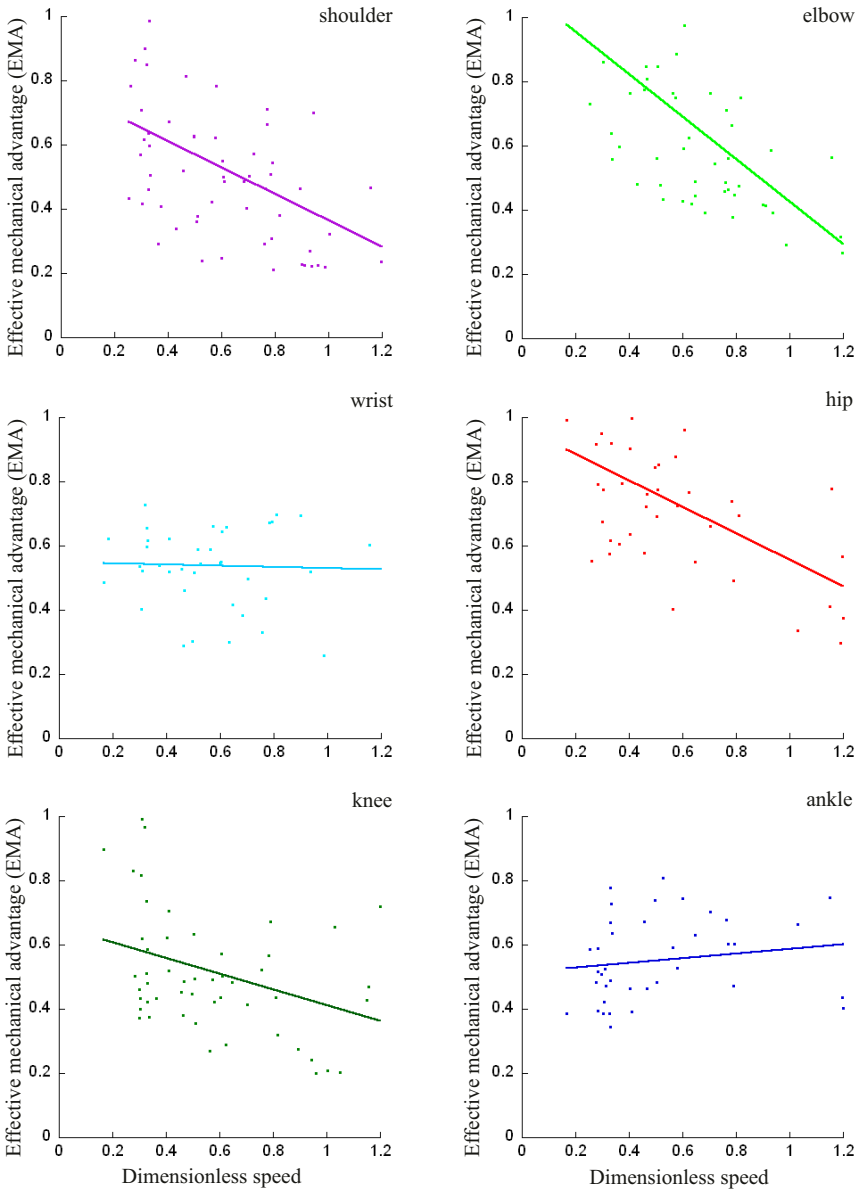

Fig. S3. EMA trends with dimensionless speed. Least squares linear regression equation data ($y = b - mx$, where b is the intercept and m is the slope) are as follows: shoulder, $n = 62$, $R^2 = 0.255$, $y = 0.777 - 0.413x$, $P < 0.01$; elbow, $n = 57$, $R^2 = 0.429$, $y = 1.09 - 0.661x$, $P < 0.01$; wrist, $n = 48$, $R^2 = 0.00214$, $y = 0.551 - 0.0219x$, $P = 0.755$; hip, $n = 45$, $R^2 = 0.396$, $y = 0.969 - 0.414x$, $P < 0.01$; knee, $n = 54$, $R^2 = 0.146$, $y = 0.658 - 0.247x$, $P < 0.01$; and ankle, $n = 40$, $R^2 = 0.0346$, $y = 0.515 + 0.0762x$, $P = 0.250$. Thus the wrist and ankle regressions are not significant at $P = 0.05$, whereas the remainder are significant.

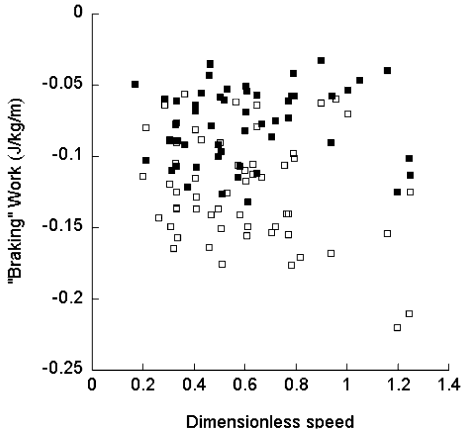

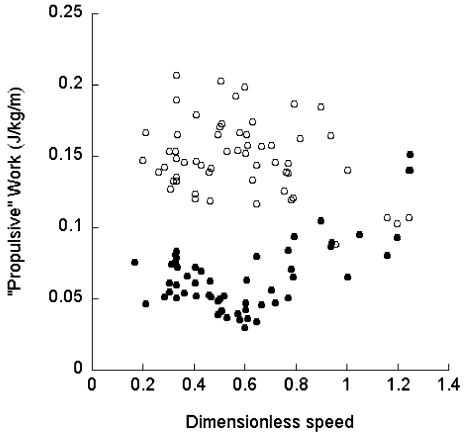

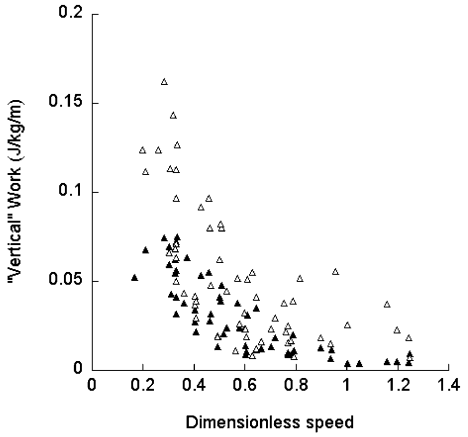

Fig. S4. Individual limb mechanical work per gait cycle versus dimensionless speed. Open symbols represent forelimbs, and closed symbols represent hindlimbs. "Propulsive" and "braking" work are respectively equivalent to the integrations of the positive and negative "horizontal" power component over a gait cycle. Some trends are evident for these horizontal components, but given the scatter in the data, we refrain from interpreting these further.

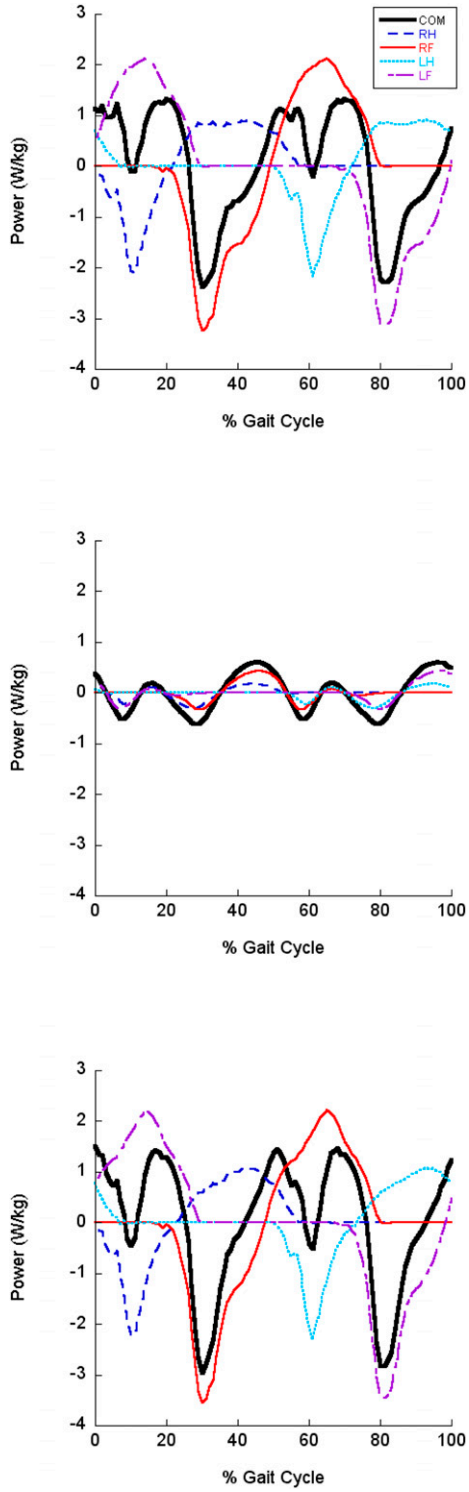

Fig. S5. Individual limb powers (means; normalized to W kg^{-1} body mass) in faster running (dimensionless speed 0.75–1.3); see Fig. 4. The gait cycle begins (0%) with the heelstrike of the right hindlimb, followed approximately by the right front (25%), left hind (50%), and left front (75%) contacts (14, 22–24). Periods of zero power correspond to swing phases of individual limbs.

Table S1. Asian elephants in Thailand: In vivo experiments

Subject	Age, years	Mass, kg	Hip height, m
Gaew	6	1984	1.52
Jojo	13	3157	1.77
Pratida	11	2984	1.69
Srisiam	5	1434	1.32
Umpang	8	1871	1.51
Wanalee	8	2318	1.32

Masses were obtained by weighing the elephants while they stood directly on the force platforms and then obtaining an average mass from two or three trials per animal. Hip heights were measured during quiet standing.

Table S2. Asian elephant cadavers: Main dissection specimens

Specimen	Age, years	Mass, kg
A	0.08	133*
B	3	835
C	22	3400
D	24	2500*
E	40	3550

Masses were obtained from truck scales (± 5 kg), except
*estimated from shoulder height (20). The mass of specimen A was very close to the three other measurements that we obtained for known-mass neonatal Asian elephants and so likely is quite reliable. The mass of specimen D was less certain but still plausible, considering the individual limb segment masses and other body dimensions, which tended to be smaller than those of the larger specimen E.

Table S3. EMA and moment arm scaling comparisons

Actual EMA*	Shoulder	Elbow	Wrist	Hip	Knee	Ankle	Mean forelimb	Mean hindlimb
Walk $\hat{u}$ =0.33	0.67	0.91	0.54	0.83	0.61	0.54	0.71	0.66
Run $\hat{u}$ =1.0	0.37	0.44	0.53	0.56	0.40	0.59	0.45	0.52
Walk/run ratio	1.78	2.05	1.03	1.50	1.53	0.91	1.58	1.28

Predicted EMA†	**Shoulder**	**Elbow**	**Wrist**	**Hip**	**Knee**	**Ankle**	**Mean forelimb**	**Mean hindlimb**	**Mean limbs**
Average	1.21	1.95	1.00	2.12	3.34	0.99	1.51	2.01	1.76
Ratio walk‡	1.75	2.07	1.80	2.44	5.23	1.80	2.07	2.93	2.50
Ratio run‡	2.86	3.90	1.74	3.32	7.14	1.56	3.01	3.44	3.22

r_{muscle}♣	**Elbow**	**Ankle**
Predicted	0.20	0.17
Ratio¶	0.69	0.36

Joint	**Muscle mass (% body mass)**	**l_{fasc} ($m^{-0.33}$)**	**r_{muscle} ($m^{-0.33}$)**
Shoulder	1.75	0.0086	0.0106
Elbow	1.24	0.0106	0.0112
Wrist	0.33	0.0070	0.0046
Hip	2.65	0.0176	0.0098
Knee	1.41	0.0121	0.0050
Ankle	0.31	0.0044	0.0050

*Mean joint EMA calculated from least squares linear regressions (Fig. S3) for the appropriate dimensionless speed, $\hat{u}$. There was considerable scatter in the data (as reported in other studies; refs. 5, 11, 12), but statistically significant speed-related trends were evident for all but the ankle and wrist joints.
†Predicted mean EMA (11) for each joint, for entire forelimb and hindlimb, and then the mean for all limbs; predictions made using the mean body mass of all subjects.
‡Ratio of predicted/actual EMA values for each joint.
♣Predicted from scaling equations (21), using mean body mass of all subjects. Units in meters.
¶Ratio of actual muscle moment arm (r_{muscle}; calculated from values below) to predicted value.

Table S4. Comparisons of locomotor cost estimates

Speed category	V_{musc}	ILM	CoM	Metabolic cost
<0.2	48.2	0.341	0.261	0.917
0.2–0.3	43.6	0.393	0.199	0.785
0.3–0.4	47.2	0.359	0.159	0.833
0.4–0.5	51.9	0.295	0.133	1.07
0.5–0.6	52.1	0.345	0.177	1.49
>0.6	63.4	0.261	0.148	1.89
Mean	51.1	0.332	0.180	1.16
SE	20.9	0.136	0.0733	0.475
B	−1.90	3.49	1.83	
M	0.0599	−7.01	−3.75	
R^2	0.884	0.575	0.157	

Units are $cm^3\ m^{-1}\ kg^{-1}$ for V_{musc} and $J\ kg^{-1}\ m^{-1}$ for the other costs. Speed categories shown are dimensionless speeds corresponding to those in Fig. 3 and data in fig. 3 in ref. 15. Estimates of cost for each speed category are shown from our calculations of muscle recruitment (V_{musc}), ILM, and CoM ("combined limb method"; ref. 19), and normalized net cost of transport data from ref. 15 applied to our subjects. The bottom three rows show the ordinary least squares linear regression equations and R^2 values, $y = b + mx$, where b is the intercept, m is the slope, y is the metabolic cost, and x is the mechanical approximation of cost. Note that the two mechanical work–based estimates (ILM and CoM) have negative slopes and thus (incorrectly) predict decreasing costs with increasing speed.

We caution that the metabolic data in ref. 15 are from African elephants, not Asian elephants, and are for different individuals than our experimental subjects (which were of generally similar mass, ~1,500 kg). Yet there is no a priori reason for this to change our fundamental conclusions that (*i*) the V_{musc} approach best fits the metabolic data, and (*ii*) the ILM work is considerably higher than the CoM work. Regardless, none of these methods is without flaws and assumptions.

Movie S1. Sample running experimental trial for elephant "Srisiam" (from Table S1), showing motion capture cameras and force platform array (as identical 2.9-MB .avi and .mov files).

Movie S1.

Movie S2. Sample running experimental trial for elephant "Srisiam" (from Table S1), showing motion capture cameras and force platform array (as identical 2.9-MB .avi and .mov files).

Movie S2.